






Cite this: *RSC Adv.*, 2018, 8, 16103

# Novel azobenzene-based amphiphilic copolymers: synthesis, self-assembly behavior and multiple-stimuli-responsive properties†

Yiting Xu, \* Jie Cao, Qi Li, Jilu Li, Kaiwei He, Tong Shen, Xinyu Liu, Conghui Yuan,   
Birong Zeng  and Lizong Dai 

A series of novel azobenzene-based amphiphilic random copolymers P(POSSMA-co-AZOMA-co-DMAEMA) were synthesized *via* reversible addition-fragmentation chain transfer (RAFT) polymerization. A light and reduction dual-responsive azo group, pH-responsive tertiary amine group and super hydrophobic POSS moiety were incorporated into the polymer chain to generate multi-stimuli-responsiveness. Self-assembly of these amphiphilic copolymers led to the formation of spherical micelles in aqueous solution. The light, pH and reduction responsive properties of the micelles were investigated systematically by DLS, TEM, UV-vis, FTIR and NMR. The azo groups can undergo *trans*–*cis* isomerization under UV light irradiation, thus causing a diameter change of the micelles. Owing to the large proportion of tertiary amine groups in amphiphiles, these micelles showed sensitive pH-response behavior. The hydrophobic azo pendant in the polymer chain completely reduced to a more hydrophilic substituted aniline in a reductive environment, resulting in the increase of overall hydrophilicity of amphiphiles and the disassembly of polymeric micelles. Owing to these multi-stimuli-responses, the polymeric micelles showed rapid and efficient release properties of hydrophobic molecules in response to pH and reductive stimuli.

Received 26th February 2018  
Accepted 25th April 2018

DOI: 10.1039/c8ra01660g  
[rsc.li/rsc-advances](http://rsc.li/rsc-advances)

## 1. Introduction

Stimuli-responsive polymeric systems integrating with special responsive moieties can undergo alteration of their chemical structures and physical properties in response to an external stimulus, such as temperature,<sup>1,2</sup> light,<sup>3,4</sup> pH<sup>5–7</sup> or reduction.<sup>8,9</sup> Azobenzene and its derivatives can undergo *trans*–*cis* isomerization under UV or vis light irradiation. Also, the azo bond is cleavable in a reducing medium, such as hydrazine (NH<sub>2</sub>NH<sub>2</sub>), sodium hydrosulfite (Na<sub>2</sub>S<sub>2</sub>O<sub>4</sub>) or azoreductase.<sup>10–12</sup> Therefore, the self-assembly behavior and the stimuli-responsive properties of azobenzene based copolymers, as well as their applications, were intensively investigated in recent years.<sup>13–17</sup> Molecules containing azobenzene moieties have the ability to form an ordered phase-separation structure in bulk, micelle, vesicles, *etc.* Unique photoresponsive properties related with the self-assembled structures have been observed and explored for potential applications in areas such as optical devices, sensors, and drug delivery.<sup>18–22</sup> Photo-responsive micelles based on azobenzene-modified amphiphilic copolymers showed

reversible self-assembly and disassembly behaviors in aqueous conditions by alternating UV and visible light irradiation. Hu<sup>23</sup> *et al.* synthesized a block copolymer poly(ethylene glycol)-modified poly(carbonate)s (PEG-*b*-poly(MPC)) and found its reversible assembly–disassembly behavior in aqueous solution triggered by visible light and UV light irradiation. Recently, an azobenzene linkage cleavable by the enzyme azoreductase or other reductants also has been reported. Rao and Khan prepared an enzyme sensitive copolymer, which can be disassembled through the cleavage of the azobenzene linkage in copolymer chain in the presence of enzyme azoreductase.<sup>24</sup> Li and coworkers prepared prodrugs of 5-aminosalicylic acid based on azobenzene molecule, and drug release can be triggered by the cleavage of azobenzene with the reduction of sodium hydrosulfite.<sup>25</sup>

Polyhedral oligomeric silsesquioxane (POSS), the well defined organic–inorganic hybrid compounds with inorganic cubic core and outer organic groups,<sup>26,27</sup> is a strong hydrophobic hybrid molecule with nanoscale dimension. POSS has attracted considerable attentions in building amphiphilic polymers due to their unique merits including nontoxic, biocompatible and chemically inert.<sup>28–31</sup> A lot of POSS-containing amphiphilic polymers have been designed and well-defined nanoaggregates have been prepared through the hydrophobic aggregation of POSS segments in aqueous solution.<sup>32,33</sup> For example, Matějka and coworkers built hybrid random copolymers containing

Fujian Provincial Key Laboratory of Fire Retardant Materials, Xiamen University, Xiamen 361005, People's Republic of China. E-mail: xyting@xmu.edu.cn; Tel: +86 18750256597

† Electronic supplementary information (ESI) available. See DOI: 10.1039/c8ra01660g



POSS moiety *via* RAFT polymerization and these amphiphilic polymers can self-assemble into spherical micelles with PMA-POSS segment as the hydrophobic part.<sup>34</sup> In this contribution, azobenzene monomer (AZOMA) was synthesized and used to prepare a series of novel azobenzene-based amphiphilic random copolymers *via* RAFT polymerization with the comonomers of methacrylate isobutyl POSS (POSSMA) and 2-(dimethylamino) ethyl methacrylate (DMAEMA). The synthesis routes of copolymer are described in Scheme 1. The incorporation of hydrophobic AZOMA and POSSMA units make it possible to self-assemble and form well-defined micelles. The hydrophobic and pH-responsive DMAEMA units can stabilize the micelles. Moreover, the introduction of azobenzene moiety and tertiary amine groups into polymer chains can endow these amphiphilic copolymers with pH-, light- and reduction-responsive properties. Based on the multi-stimuli-responsiveness of polymeric micelles, Nile red was selected as a hydrophobic molecular model to study the guest molecular encapsulation and release abilities of copolymers.

## 2. Experimental

### 2.1 Materials

Methacrylate isobutyl POSS (POSSMA) was obtained from Hybrid Plastic Co. (USA) and used without further purification. 2-(Dimethylamino)ethyl methacrylate (DMAEMA) was purchased from Aladdin Chemical Co. Ltd. (Shanghai, China). *N*-Ethyl-*N*-hydroxyethylamine (96%) and the RAFT agent cumyldithiobenzoate (CDB) was purchased from J&K Chemical Ltd. (Shanghai, China). Aniline and sodium dithionite were purchased from Sinopharm Chemical Reagent Co. Ltd. (Shanghai, China). Azobisisobutyronitrile (AIBN) was recrystallized from ethanol. All reagents in analytical grade were used as received, unless otherwise have been noted before.

### 2.2 Synthesis of azobenzene monomer (AZOMA)

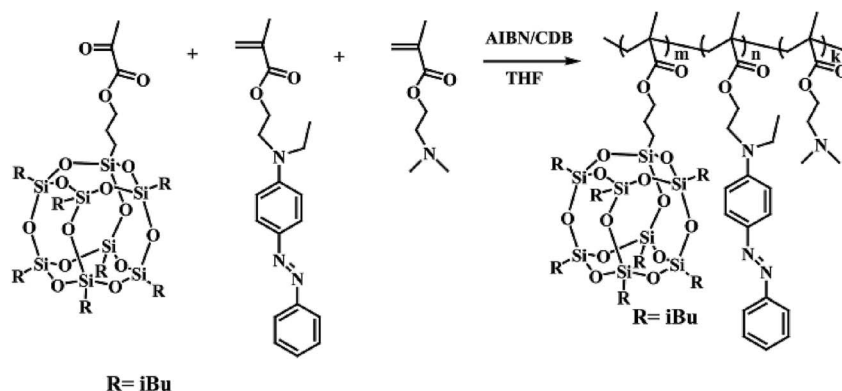
The synthetic route of the monomer AZOMA was illustrated literature, according to the procedure similar to the published method.<sup>35</sup> A solution of aniline (2.3280 g, 25 mmol) in concentrated HCl aqueous solution (60 mL, 20 vol%) was cooled

to 0 °C, and NaNO<sub>2</sub> (1.8975 g, 27.5 mmol) in water (20 mL) was added slowly. The mixture was stirred for 15 min in an ice bath to obtain a solution of diazonium salt, AZO-N<sub>2</sub><sup>+</sup>, which was then added to a solution of 2-(*N*-ethylanilino)ethanol (4.1308 g, 25 mmol) in acetic acid aqueous solution (30 mL, 30 vol%). After 5 min, K<sub>2</sub>CO<sub>3</sub> aqueous solution (10 wt%) was added to adjust the pH value to 7. After filtration, the resulting solid was purified by column chromatography (gel silica gel, *n*-hexane : ethyl acetate, 1 : 1). Finally, the product was dried in a vacuum at room temperature for 12 h to afford 4.95 g (74%) of product. The structure of HOAZO was characterized by FTIR and <sup>1</sup>H NMR and ESI-MS spectroscopies. <sup>1</sup>H NMR (400 MHz d<sub>6</sub>-DMSO, δ in ppm) in Fig. S1:† 7.77 (4H), 7.52 (2H), 7.42 (1H), 6.83 (2H), 4.83 (1H), 3.58 (2H), 3.50 (4H), 1.14 (3H). The molecular weight of 269 (C<sub>16</sub>H<sub>19</sub>N<sub>3</sub>O) is consistent with the molecular ion peak [M + H]<sup>+</sup> in Fig. S2.†

A solution of 4'-[2-(hydroxyethyl)ethylamino] azobenzene HOAZO (2.6934 g, 10 mmol) and triethylamine (2.0238 g, 20 mmol) were dissolved in dichloromethane (100 mL). A solution of methacryloyl chloride (1.5680 g, 15 mmol) in dichloromethane (15 mL) was added slowly to the above mixture in an ice bath. The resultant mixture was stirred for 24 h at ambient temperature. The solution was washed with the saturated solution of NaCl, and the organic phase was dried over anhydrous MgSO<sub>4</sub>. The solvent was removed by rotary evaporation and the residue was purified by column chromatography (gel silica gel, *n*-hexane : ethyl acetate, 1 : 5). Finally, the product was dried in a vacuum at room temperature for 12 h. A yield of 82% was obtained. <sup>1</sup>H NMR (d<sub>1</sub>-CDCl<sub>3</sub>, δ in ppm) in Fig. S3:† 7.86 (4H), 7.47 (2H), 7.38 (1H), 6.80 (2H), 6.11 (1H), 5.58 (1H), 4.36 (2H), 3.70 (2H), 3.52 (2H), 1.95 (3H), 1.24 (3H). The result of ESI-MS analysis for AZOMA is shown in Fig. S4.† The molecular weight of 337 (C<sub>20</sub>H<sub>23</sub>N<sub>3</sub>O<sub>2</sub>) is consistent with the molecular ion peak [M + H]<sup>+</sup> in Fig. S4.†

### 2.3 Synthesis of azobenzene-based copolymers P(POSSMA-co-AZOMA-co-DMAEMA)

Azobenzene-based copolymer, P(POSSMA-co-AZOMA-co-DMAEMA), were synthesized with monomers of AZOMA, POSSMA and DMAEMA *via* RAFT polymerization as shown in



Scheme 1 Synthesis of copolymer of P(POSSMA-co-AZOMA-co-DMAEMA).



Scheme 1. The RAFT polymerization was followed: AZOMA (0.6748 g, 2.0 mmol), POSSMA (0.4526 g, 0.48 mmol), DMAEMA (0.6288 g, 4.0 mmol), CDB (0.0109 g, 0.04 mmol), and AIBN (0.0013 g, 0.008 mmol) were added into the Schlenk tube with 3.0 mL of THF. The polymerization ampoule was degassed with five freeze–pump–thaw cycles. Then the Schlenk tube was filled with argon and placed in an oil bath at 65 °C for 48 h. The reaction was stopped into liquid nitrogen. Then the product was precipitated in excess hexane, and washed with hexane three times. The resulting red powder was dried overnight under vacuum at room temperature.

FTIR (KBr, wavenumber in  $\text{cm}^{-1}$ ) (Fig. S6†): 2953, 2821, 2770, 1728, 1600, 1513, 1462, 1399, 1135, 1017, 962, 822, 766, 746, 690.  $^1\text{H}$  NMR ( $\text{d}_1\text{-CDCl}_3$ ,  $\delta$  in ppm) (Fig. S7†): 7.82 (s, 4H), 7.45 (s, 2H), 7.36 (s, 1H), 6.78 (s, 2H), 4.04 (s, 2H), 3.86 (m, 2H), 3.62 (s, 2H), 3.48 (s, 2H), 2.54 (s, 2H), 2.26 (s, 3H), 1.84 (d, 2H), 0.59 (d, 16H).

#### 2.4 Synthesis copolymers of P(POSSMA-co-DMAEMA), P(AZOMA-co-DMAEMA), P((POSSMA-co-AZOMA)-b-DMAEMA) and P(POSSMA-co-AZOMA-co-DMAEMA) as control samples

As control samples, P(AZOMA-co-DMAEMA), P(POSSMA-co-DMAEMA), P(POSSMA-co-AZOMA)-b-P(DMAEMA) were synthesized by RAFT polymerization, and random copolymers of P(POSSMA-co-AZOMA-co-DMAEMA) was prepared by conventional free radical polymerization. Their synthetic process was provided in ESI.† The copolymers were characterization by  $^1\text{H}$  NMR spectra (Fig. S7†) and GPC (Fig. S8†).

#### 2.5 Preparation of copolymer micelles in aqueous solution

P(POSSMA-co-AZOMA-co-DMAEMA) random copolymers and control samples and were dissolved in THF. Then predetermined volume Milli-Q water, which is a selective solvent for copolymers, was added into the solution at the speed of  $1.0 \text{ mL min}^{-1}$ , to induce the self-assembly of copolymer. Afterwards, the mixture was stirred for 3 days at ambient temperature to remove the THF.

#### 2.6 Preparation and characterization of Nile red-loaded micelles

P(POSSMA-co-AZOMA-co-DMAEMA) random copolymers and Nile red were dissolved in THF. Then predetermined volume Milli-Q water was added into above solution to induce the self-assembly of P(POSSMA-co-AZOMA-co-DMAEMA) and load Nile red molecule. Afterwards, the solution was dialysis against Milli-Q water using a dialysis membrane with a molecular weight cutoff of 3000 Da for 2 days. The standard solutions of Nile red were also prepared to build standard work curve. The incorporation efficiency (IE) and loading capacity (LC) were calculated using below equations.

$$\text{LC}\% = \frac{\text{encapsulated molecule mass}}{\text{total molecule mass}}\%$$

$$\text{IE}\% = \frac{\text{encapsulated molecule mass}}{\text{polymeric micelle weight} + \text{encapsulated molecule mass}}\%$$

#### 2.7 Characterization

$^1\text{H}$  NMR spectra were recorded on a Bruker AV400 MHz NMR spectrometer using  $\text{d}_1\text{-CDCl}_3$  and  $\text{d}_6\text{-DMSO}$  as the solvent. FTIR measurements were conducted on an AVATAR 360 FTIR (Nicolet Instrument) at room temperature. Molecular weight determinations for monomers were conducted on an Esquire 3000 plus mass spectrometer (Bruker Daltonics) and the solvent was methanol at the concentration of  $1 \text{ mg mL}^{-1}$ . Molecular weight determinations for polymers were made using GPC analyses performed in THF using a series of waters styragel HR2, HR4, and HR5. The eluent was THF at a flow rate of  $1.0 \text{ mL min}^{-1}$ . A series of low polydispersity polystyrene standards were used for the GPC calibration. Dynamic Light Scattering (DLS) measurements were used to measure the zeta potential, aggregate size and size distribution and performed on a Zetasizer Nano ZS Instrument (Malvern Instruments, UK) at a scattering angle of  $90^\circ$ , and analyzed by Malvern Zetasizer software version 6.20. Transmission Electron Microscopy (TEM) analysis was performed on a JEM2100 transmission electron microscope with an accelerating voltage of 200 kV. One drop of micelles solution was placed on a copper-mesh coated with carbon and then air-dried before measurement. The UV-vis spectra of P(POSSMA-co-AZOMA-co-DMAEMA) micellar solutions at various condition were measured using a UV-2550 spectrometer (SHI-MADZU). The fluorescence emission spectra were measured using a Horiba Fluoromax-4.

### 3. Results and discussion

#### 3.1 Synthesis of azobenzene-based copolymer

Azobenzene-based copolymer, P(POSSMA-co-AZOMA-co-DMAEMA), AZOMA, POSSMA and DMAEMA via RAFT polymerization were shown in Scheme 1. Table 1 summarizes the results obtained for copolymers with different ratio of the monomers to CDB. Three types of P(POSSMA-co-AZOMA-co-DMAEMA)s denoted as RCP-1, RCP-2 and RCP-3 were prepared, the molecular weights of which are  $1.375 \times 10^4$  (PDI = 1.17),  $1.973 \times 10^4$  (PDI = 1.26),  $2.175 \times 10^4$  (PDI = 1.30) (Fig. S10†), respectively. Control samples of P(AZOMA-co-DMAEMA), P(POSSMA-co-DMAEMA) and P(POSSMA-co-AZOMA)-b-P(DMAEMA) were synthesized by RAFT polymerization denoted as C-1, C-2, C-3, and P(POSSMA-co-AZOMA-co-DMAEMA) was prepared by conventional free radical polymerization denoted as C-4. Their experimental conditions and results were also shown in Table 1.

FTIR and NMR are also applied to characterize the copolymer, the results of which are shown in Fig. S6 and S7.† The absorption peaks at around  $2821 \text{ cm}^{-1}$  and  $2770 \text{ cm}^{-1}$  are attributed to  $-\text{NCH}_3$  and  $-\text{NCH}_2-$  in DMAEMA units. Compared to AZOMA monomer, we assign the broad absorption peak at  $1115 \text{ cm}^{-1}$  to overlapping peaks of C–N bond in AZOMA units and Si–O–Si bond in POSSMA units. In Fig. S8,† there are no NMR signals in



**Table 1** Experimental conditions and results of the RAFT or conventional free radical polymerization to obtain copolymers of P(POSSMA-co-AZOMA-co-DMAEMA) or control samples<sup>a</sup>

Sample	[POSSMA] : [AZOMA] : [DMAEMA] : [CDB] : [AIBN] <sup>a</sup>	[POSSMA] : [AZOMA] : [DMAEMA] <sup>b</sup>	Time (h)	10 <sup>-3</sup> <i>M<sub>n</sub></i> (GPC)	PDI	Polymer yield
RCP-1	12 : 50 : 100 : 1.25 : 0.25	0.17 : 1.0 : 1.9	48	11.78	1.17	63.2%
RCP-2	12 : 50 : 100 : 1.00 : 0.20	0.16 : 1.0 : 2.1	48	15.55	1.26	66.1%
RCP-3	12 : 50 : 100 : 0.75 : 0.15	0.18 : 1.0 : 2.2	48	16.66	1.30	59.4%
C-1	0 : 50 : 100 : 1.00 : 0.20	0 : 1.0 : 2.27	48	11.4	1.27	47.7%
C-2	12 : 0 : 100 : 1.00 : 0.20	1.0 : 0 : 7.76	48	9.43	1.22	56.2%
C-3 <sup>c</sup>	12 : 50 : 100 : 1.00 : 0.20	0.18 : 1.0 : 2.93	48	18.6	1.34	51.3%
C-4	12 : 50 : 100 : 0 : 1.00	0.21 : 1.0 : 2.56	48	19.3	2.32	41.3%

<sup>a</sup> The feed molar ratio of monomers, the chain transfer agent and initiator. <sup>b</sup> The composition ratio in copolymer chains determined from <sup>1</sup>H-NMR spectra by the integral areas of characteristic peak relevant to every structural unit. For example, the composition ratio of RCP-1 was calculated as [POSSMA] : [AZOMA] : [DMAEMA] =  $A_{0.59}/16 : A_{7.82}/4 : A_{2.26}/6$ , in which *A* was areas for short. <sup>c</sup> Block copolymer C-3 is synthesized by RAFT polymerization using P(POSSMA-co-AZOMA) as macromolecular chain transfer agent with feed molar ratio of [P(POSSMA-co-AZOMA)] : [DMAEMA] : [AIBN] = 1 : 100 : 0.20, and P(POSSMA-co-AZOMA) macromolecular chain transfer agent is synthesized with feed molar ratio of [POSSMA] : [AZOMA] : [CDB] : [AIBN] = 12 : 50 : 1.00 : 0.20.

the  $\delta$  range of 5.5 to 6.5 ppm, which belongs to vinyl protons in monomers, indicating that the purification by precipitation removes the residual monomers. The signals of the aromatic ring protons at 7.82 ppm for AZOMA units and the methyl protons in tertiary amine of DMAEMA units at 2.26 ppm and the methylene protons next to silicon in POSSMA units at 0.59 ppm demonstrate that three monomers are introduced into the copolymer chains as expected. The relative ratio of POSSMA, AZOMA and DMAEMA units in copolymer chains can be determined by calculating the integral ratio among the characteristic signal peaks in Fig. S11.† The ratio of three azobenzene-based copolymer [POSSMA] : [AZOMA] : [DMAEMA] is 0.17 : 1.0 : 1.9, 0.16 : 1.0 : 2.1 and 0.18 : 1.0 : 2.2, respectively.

### 3.2 The morphology of P(POSSMA-co-AZOMA-co-DMAEMA) self-assembly aggregates in aqueous solution

A typical TEM image of the micelles formed by RCP-2 with a concentration of 2.5 mg mL<sup>-1</sup> (pH = 6.9, 25 °C) in aqueous solution is presented in Fig. 1a. The micelles display spherical

shapes with a well-defined core-shell structure, in which hydrophobic POSSMA and AZOMA is as cores and hydrophilic DMAEMA as shells. The hydrophobic effect of POSS moieties and  $\pi$ - $\pi$  stacking effect of AZO moieties induce molecular chain aggregate in water. The hydrogen bonds between DMAEMA and water, and the protonated DMAEMA in weakly acidic Milli Q water stabilize the aggregates. And the zeta potential of the micellar solution is +5.92 mV. It is indicated that micelle surface charges are positive. The <sup>1</sup>H NMR spectrum of micelles of random copolymer in D<sub>2</sub>O is shown in Fig. S12,† in which only special peaks for DMAEMA are displayed: 1.75 ppm for -N(CH<sub>3</sub>), 3.25 ppm for -N(CH<sub>2</sub>), 3.75 ppm for -O(CH<sub>2</sub>). It is further that the shell of micelles consists of DMAEMA. The large hydrophobic core volume might be resulted from the aggregation of POSS moieties in polymer side chains, which have nature nanoscale at about 1.5 nm and neat space structure. The characteristic structure makes micelles more advantageous in encapsulating of hydrophobic drugs. The DLS result in Fig. 1b indicates that the micelles have an average diameter of 155.5 nm with a size distribution of PDI = 0.156. The difference between the sizes measured by DLS and determined by TEM can be attributed to the fact that the DLS measures swollen micelles in aqueous solutions, and the sizes observed by TEM are derived from the dried micelles. The micellization process of the copolymer is shown in Fig. 1c.

In order to clarify the formation of the assembled structures from amphiphilic random copolymer of P(POSSMA-co-AZOMA-co-DMAEMA), some control samples self-assembly aggregates are also studied. Their SEM photos are shown in Fig. 2. The C-1 can self-assemble in water to form spherical micelles with hydrophobic AZOMA as cores and hydrophilic DMAEMA as shells. But the aggregates of C-2 is irregular, which is because the ratio of hydrophobic POSSMA moieties to too less than AZOMA in C-1, and there is no appropriate hydrophilic-hydrophobic balance in C-2 to form spherical micelles. The micelles of C-3 are uniform due to its narrow dispersity in both molecular weight and block length. The C-4 also can self-assemble in water to form spherical micelles with a broad dispersion of size

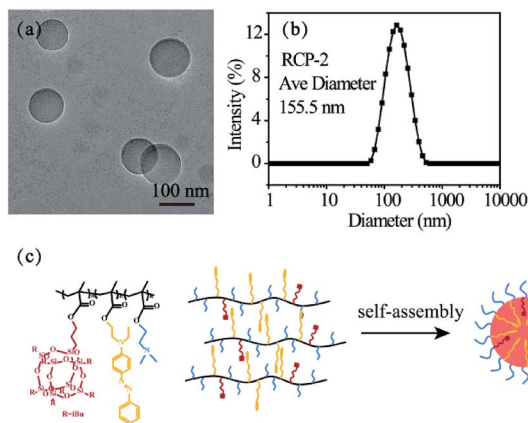


**Fig. 1** TEM image (a) and DLS result (b) of 2.5 mg mL<sup>-1</sup> RCP-2 micelles (pH = 6.9, 25 °C) and schematic representation for the self-assembly process of P(POSSMA-co-AZOMA-co-DMAEMA) (c).





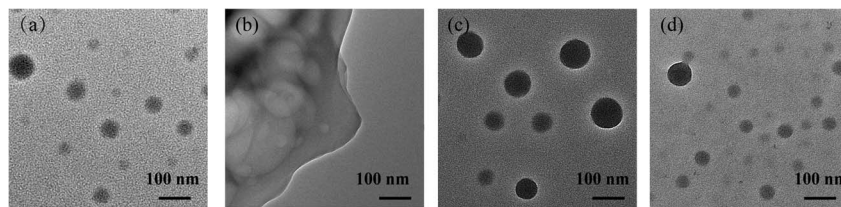


Fig. 2 TEM images of control samples, (a) P(AZOMA-DMAEMA), (b) P(POSSMA-co-DMAEMA), (c) P(POSSMA-co-AZOMA)-*b*-P(DMAEMA) by RAFT, (d) P(POSSMA-co-AZOMA-co-DMAEMA) by conventional free radical polymerization.

distribution. It is because that molecular weight of C-4 *via* conventional free radical polymerization has a broader polydispersity than that of controlled RAFT polymerization. According to the self-assembly behaviors of control samples, we know that amphiphilic random copolymers can form micelles, and there are many factor influence its morphology. Copolymer composition is an important factor in the process of self-assembly of random copolymers. Self-assembly of random copolymers is largely dependent on their hydrophilic-hydrophobic balance (often referred to as the hydrophilic-lipophilic balance (HLB)).<sup>36</sup>

The initial concentration of amphiphilic copolymer is one of important factors in the self-assembly process, which influences the morphology and size of self-assembled aggregates. The RCP-2 micelles at different initial concentration. As shown in Fig. 2, the diameter of micelles with  $1.0 \text{ mg mL}^{-1}$ ,  $2.5 \text{ mg mL}^{-1}$  and  $5.0 \text{ mg mL}^{-1}$  is  $121.1 \text{ nm}$  ( $\text{PDI} = 0.160$ ),  $155.5 \text{ nm}$  ( $\text{PDI} = 0.156$ ) and  $196.4 \text{ nm}$  ( $\text{PDI} = 0.178$ ), respectively. This increase of micellar diameter induced by initial concentration is also observed in the TEM images in Fig. 3. Furthermore, the increase of initial concentration results in the increase the number of micelles and deformation of micelles, but does not change the core-shell structure of micelle.

We also prepared micellar solution of RCP-1, RCP-2 and RCP-3 at the concentration of  $2.5 \text{ mg mL}^{-1}$ , whose sizes and size distributions are shown in Fig. 3. In the case of RCP-1, the size of micelles is  $106.0 \text{ nm}$ . And the size increase to  $155.5 \text{ nm}$  and  $176.4 \text{ nm}$  for RCP-2 and RCP-3, respectively. TEM images confirm this trend that the micelle size increased as  $M_w$  increasing. This result derived from that the more hydrophobic molecular with higher  $M_w$ , a larger micelles in size should be formed to achieve hydrophobic balance.

The critical micelle concentrations (CMC) of RCP-1, RCP-2 and RCP-3 are also measured by a fluorescence method with hydrophobic Nile red as a fluorescent probe. Fluorescence spectroscopy ( $\lambda_{\text{ex}} = 560 \text{ nm}$ ) is utilized to monitor the self-assembly process. The CMC of RCP-1, RCP-2 and RCP-3 is found to be  $0.258 \text{ mg mL}^{-1}$ ,  $0.239 \text{ mg mL}^{-1}$  and  $0.181 \text{ mg mL}^{-1}$ , respectively. Despite the three units ratio is pretty similar in RCP-1, RCP-2 and RCP-3, the increase in molecular weight will improve the hydrophobicity of the whole polymer chains. Furthermore, the longer polymer chain length possesses the stronger intermolecular interaction. These factors can increase the driving force of self-assembly process, which means that this amphiphilic copolymer can form micelles at a lower concentration.

### 3.3 Light-responsive properties of P(POSSMA-co-AZOMA-co-DMAEMA) micelles

Fig. 3a shows the hydrodynamic radius of RCP-2 micelles at  $1.0 \text{ mg mL}^{-1}$  upon light irradiation at  $365 \text{ nm}$ . After UV light irradiation, the sizes of micelles decrease in the first 5 min, and then remain unchanged. It can be explained from the *trans-cis* isomerization of the azo moieties, which results in the decrease of molecular size and form a more compact aggregate in the core of micelles. The UV-vis absorption spectra before and after the irradiation of UV light are shown in Fig. 4b. The absorption of  $\pi-\pi^*$  transition band of typical aminoazobenzenes at  $414 \text{ nm}$  reduced rapidly after 1 min of UV light irradiation, and substantially retained the same value. It indicates the isomerization of azo groups from *trans* configuration to *cis* configuration and the photoisomerization reaches a balance state in a short time. Due to the transition band of  $\pi-\pi^*$  and  $n-\pi^*$  is close, the  $n-\pi^*$  might be completely buried beneath the intense  $\pi-\pi^*$ , one could not identify the absorption of azo-group in *cis* configuration.

### 3.4 pH-responsive properties of P(POSSMA-co-AZOMA-co-DMAEMA) micelles

There are subtle differences in the acid-base properties of human tissues, for example, the pH value ranges from 1 to 2 in the stomach, 8 to 9 in the small intestine, and the pH value drops to 5.8–7.2 in tumor tissues due to the production of lactic acid. According to this difference in pH, pH-responsive assemblies and drug delivery systems can be designed to achieve site-specific drug release and enhance the utilization of drugs by control pH value. Incorporation of pH-responsive DMAEMA units into a polymer chains endows the polymeric micelles with pH-response property. The pH dependence of the aggregates for RCP-2 solution ( $2.5 \text{ mg mL}^{-1}$ ) is examined by DLS and TEM. The results are revealed in Fig. 5c and d, the changes of aggregates can undergo two stages with the variation of pH. The micellar size remarkably increases from  $154.4$  to  $216.5 \text{ nm}$  when pH decreases from 6.9 to 6.0. As shown in Fig. 5a and b, the clear shell-core spherical structure can be identified when pH value is 6.5. However, when pH value further decreases to 6.0, the spherical structure of micelle has been destroyed and formed irregular polymer aggregates. When pH is further decreased to 5.5, the size distribution of aggregate is much broader ( $\text{PDI} = 0.475$ ) and the main peak is about  $10\text{--}15 \text{ nm}$ , which indicates that polymeric micelles have been disassembled. This increase in aggregate size in the pH range of



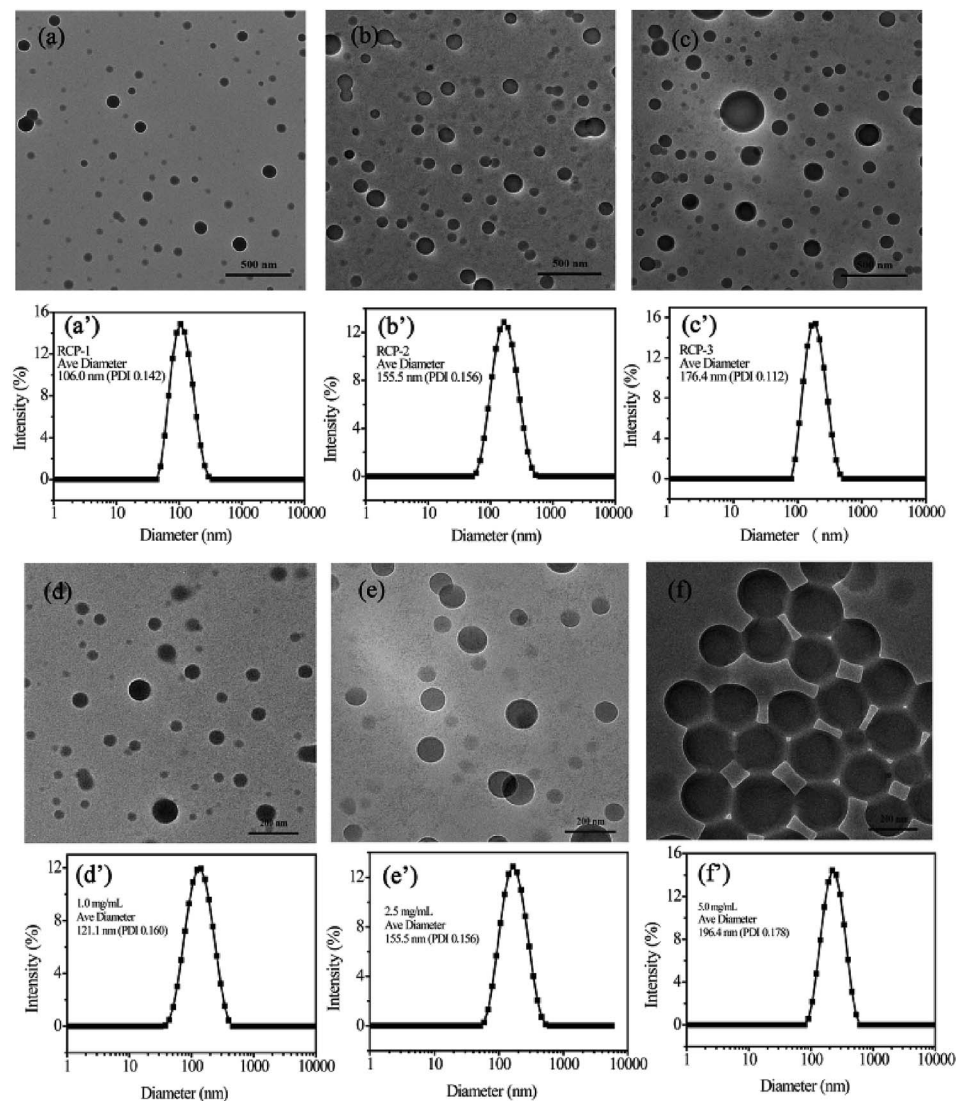


Fig. 3 TEM images (a)–(c) and DLS results (a')–(c') of RCP-1, RCP-2 and RCP-3, TEM images (d)–(f) and DLS results (d')–(f') of RCP-2 micelles at various initial concentration of 1.0 mg mL<sup>-1</sup>, 2.5 mg mL<sup>-1</sup> and 5.0 mg mL<sup>-1</sup>.

6.9–6.0 can be ascribed to the higher degree of protonation and molecular repulsion of the DMAEMA unites. The decrease in aggregate size at pH 5.5 may derive from the disruption of hydrophilic–hydrophobic balance of P(POSSMA-*co*-AZOMA-*co*-

DMAEMA) copolymer with a large proportion of protonated DMAEMA units (about 63.29 mol%). Further, the tertiary amino groups in AZOMA units can also be protonated in an acidic solution. These structural factors endow P(POSSMA-*co*-AZOMA-

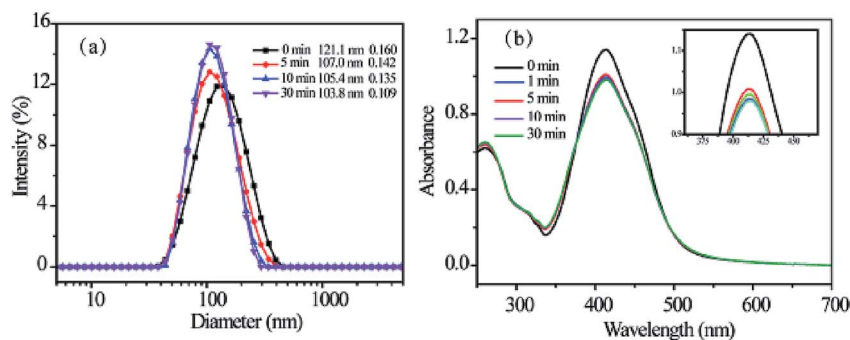


Fig. 4 The change in size of RCP-2 micelles upon irradiation of UV light (a) and the change in their UV-vis spectra (b).



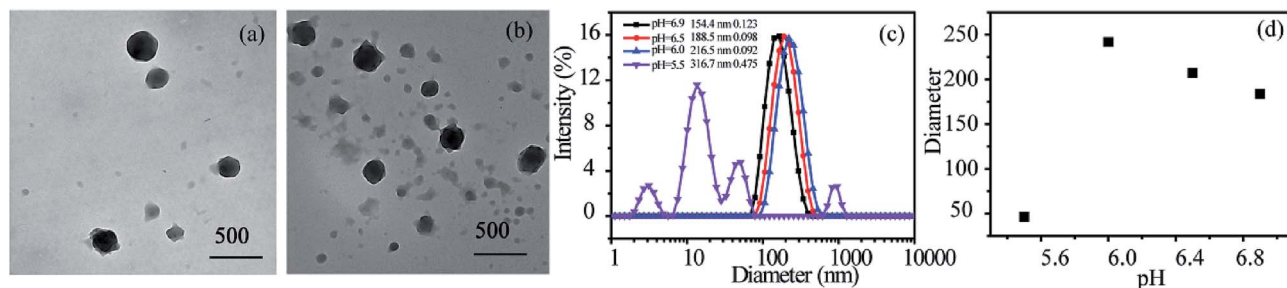


Fig. 5 TEM images of micelles at various pH: (a) pH = 6.5, (b) pH = 6.0, and diameters (c) and trend (d) of self-assembly micelles at various pH.

*co*-DMAEMA) micelles with sensitive pH-response property, which slightly changes in pH value can induce significant changes in the polymer's aggregates. It also can be found that the aggregates are deformed and the core-shell structure disappear in the TEM photos in Fig. 7. There are even a large number of residual irregular polymer aggregates for the disassembly of micelles when pH is 6.0. Fig. 7c describes the pH-induced micellization behavior of P(POSSMA-*co*-AZOMA-*co*-DMAEMA).

### 3.5 Reduction-responsive property of micelles

Azobenzene moiety is a dual-responsive moiety to ultraviolet light irradiation and reductive environment. Sodium dithionite ( $\text{Na}_2\text{S}_2\text{O}_4$ ) is selected as reductant to investigate the reduction-responsive property of P(POSSMA-*co*-AZOMA-*co*-DMAEMA) micelles. UV-vis spectroscopy is used to monitor the change of

the UV-vis absorption intensity of P(POSSMA-*co*-AZOMA-*co*-DMAEMA) micelles upon the addition of reductant  $\text{Na}_2\text{S}_2\text{O}_4$ . As shown in Fig. 6a, with the addition of  $\text{Na}_2\text{S}_2\text{O}_4$ , the absorption of *trans* azobenzene (416 nm) decreases significantly and eventually disappears, which indicates that azo pendant in polymer chain completely cleavages. For this reason, the yellow micellar solution turns colorless (Fig. 6a). DLS data shows that micelle particle size increased to 189.9 nm upon adding  $\text{Na}_2\text{S}_2\text{O}_4$  aqueous solution. The spherical micelles with core-shell structure were completely deformed to irregular nano-aggregates (Fig. 6b and c), indicating that polymer micelles have been disassembled. This micelle morphology transition can be attributed to the fact that azo pendant in polymer chain completely reduced to the corresponding cleaved product after adding 10 mg  $\text{Na}_2\text{S}_2\text{O}_4$  (Fig. 7a). The cleaved product, namely substituted aniline, shows more hydrophilic than azopendant

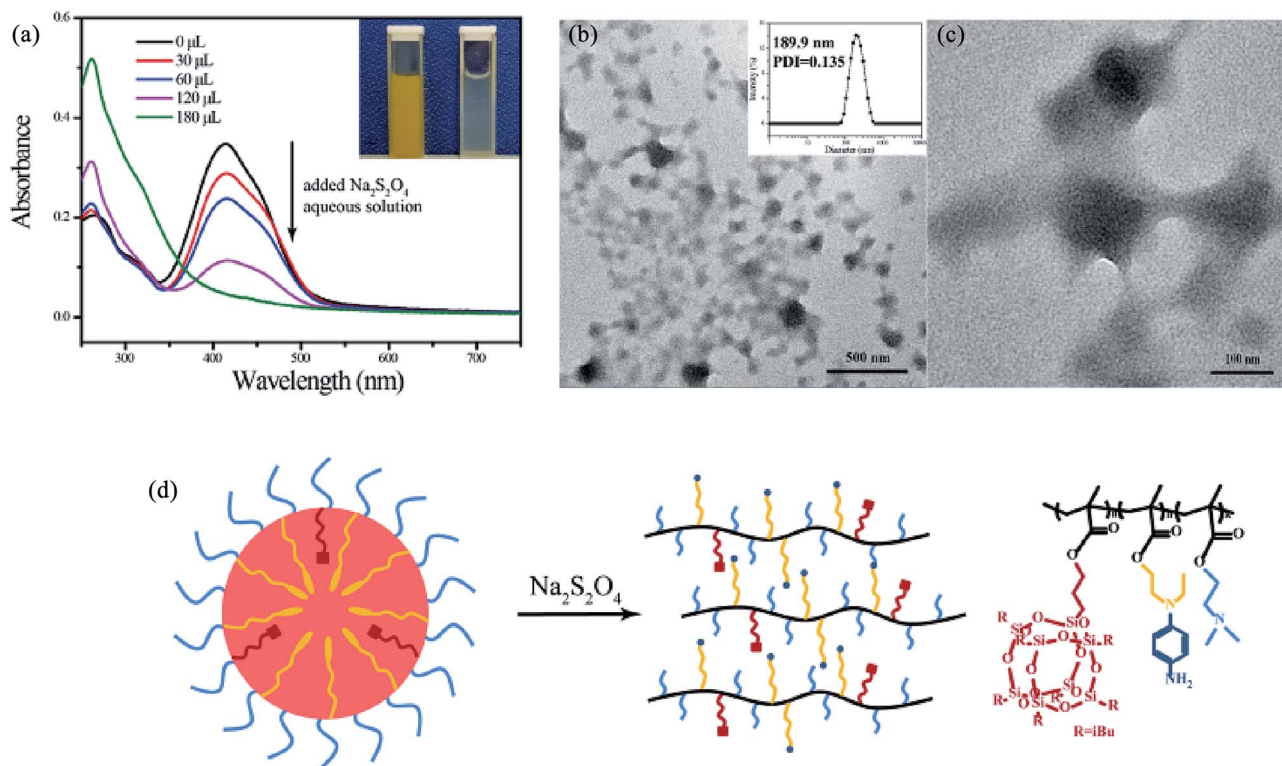


Fig. 6 UV-vis spectra and photograph of RCP-2 micelles solution upon reduction of  $\text{Na}_2\text{S}_2\text{O}_4$  and the inset of (a) represents the photograph of micelles solution, and their TEM images (b) and (c) and the inset of (b) represents DLS data, (d) simulate images of RCP-2 micelles solution upon reduction of  $\text{Na}_2\text{S}_2\text{O}_4$ .





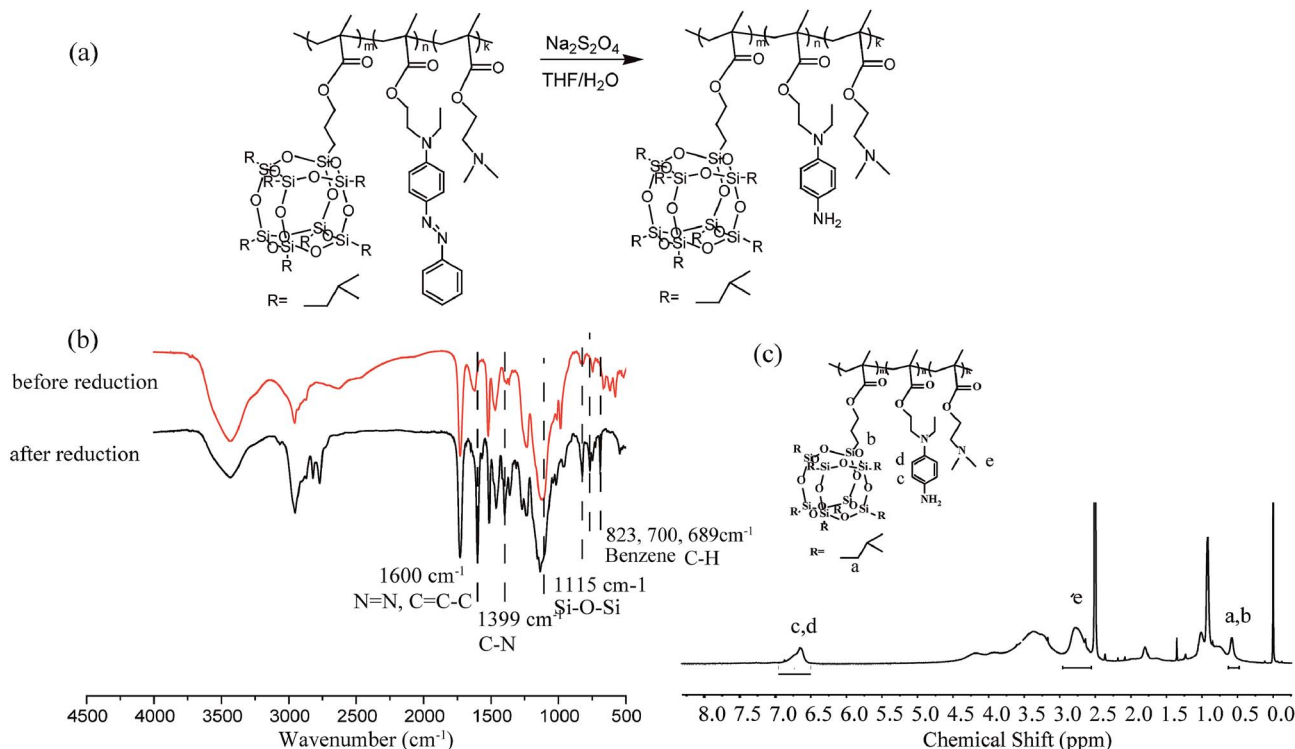


Fig. 7 Reduction reaction of P(POSSMA-co-AZOMA-co-DMAEMA) (a) and the FTIR spectra of RCP-2 and product after reduction of  $\text{Na}_2\text{S}_2\text{O}_4$  (b) and the  $^1\text{H}$  NMR of product after reduction of  $\text{Na}_2\text{S}_2\text{O}_4$  (c).

and the proportion of AZOMA units in copolymer is about 31.65 mol%, resulting the disruption of hydrophilic-hydrophobic balance of P(POSSMA-co-AZOMA-co-DMAEMA) copolymer in solution. Due to the formation of hydrogen bonds between the substituted aniline and water and the strong hydrophobic POSSMA units (about 5.06 mol%), the polymeric micelles deformed into irregular nano-aggregates. This analysis is based on the reduction reaction of P(POSSMA-co-AZOMA-co-DMAEMA) copolymer. So, it is necessary to analyze the cleaved product of copolymer.  $\text{Na}_2\text{S}_2\text{O}_4$  is selected as reductive agent to get the cleaved product of copolymer and  $^1\text{H}$  NMR and FT-IR are used to analysis the structure of the product for micelle solution treated by  $\text{Na}_2\text{S}_2\text{O}_4$ . The FTIR spectrum of RCP-2 has been changed significantly after reduction (Fig. 7b). Owing to the cleavage of azo bond, half of benzene ring in azobenzene moiety is separated from the end of the side chain. As a result, the overlapping peaks at about  $1600\text{ cm}^{-1}$  is significantly weakened, which attributes to the benzene ring skeleton vibration and the azo bond vibrations. At the same time, the absorption of C-N bond at about  $1399\text{ cm}^{-1}$  is significantly reduced. In addition, C-H deformation vibration on the phenyl ring characteristic peak have also been significantly changed. After the reduction of 1,4-substituted benzene ring the characteristic peaks at  $823\text{ cm}^{-1}$ ,  $770\text{ cm}^{-1}$  and  $689\text{ cm}^{-1}$  for mono-substituted benzene ring disappear. However, C-H characteristic absorption of 1,4-substituted benzene peak at  $749\text{ cm}^{-1}$  still exists.

We can clearly distinguish the signals of three structures units in the reduced product of RCP-2, whose  $^1\text{H}$  NMR spectrum

( $\text{d}_6$ -DMSO) is shown in Fig. 7c. The signals of protons in  $-\text{SiH}_2-$  of POSSMA units at 0.58 ppm (16H), the protons of in  $-\text{NCH}_3$  of DMAEMA units at 2.78 ppm (6H) and the peaks at  $\delta = 6.66\text{ ppm}$  (4H) correspond to the protons of the benzene ring for substituted aniline. The signals of the protons of in benzene units shift from 7.82, 7.36 to 6.7 ppm, and their integral area ratio decrease in comparison with RCP-2. By integrating these three peaks, it can be calculated that [POSSMA] : [AZOMA] : [DMAEMA] ratio is 0.17 : 1.0 : 2.2, which is similar to and the ratio of 0.16 : 1.0 : 2.1 for the copolymer before reduction. Accordingly to these structural analysis to the reduced product, we confirm that the azobenzene-based amphiphiles can be cleaved in azobenzene moiety and this reduction process will not affect the main chain of polymer. Since the hydrophobic azobenzene side strand breaks to form a more hydrophilic side groups of substituted aniline, the copolymer transforms to a more hydrophilic macromolecule and induces the disassembly of micelles.

### 3.6 Control release property of micelles

Multi-responsive polymeric micelles with core-shell structure is a good candidate for encapsulating and releasing hydrophobic guest molecules, in which the hydrophobic core can provide a large space for encapsulating guest molecules and the hydrophilic shell can provide protect the encapsulated molecules. What's more, the encapsulated molecules can be released upon the changes of environment. Given P(POSSMA-co-AZOMA-co-DMAEMA) micelles have a greater volume of the hydrophobic





**Table 2** IE and LC of Nile red in copolymer micellar solution (1.0 mg mL<sup>-1</sup>)

Sample	IE (%)	LC (%)
RCP-1	31.25	23.1
RCP-2	36.42	28.01
RCP-3	40.73	33.25

core and a good pH and reducing response characteristics, the encapsulating and release properties of micelles are discussed.

Nile red was selected as a hydrophobic molecular model to study the properties of encapsulating and releasing hydrophobic molecules in response to the pH and reductive stimulus. The copolymer micelles encapsulated Nile red were prepared, IE and LC of Nile red in copolymer micelles was determined by fluorescence spectroscopy with excitation wavelength of 490 nm and the emission intensity at 620 nm. The standard work curve is built with correlation coefficient ( $R^2$ ) value at least 0.999

(Fig. S14<sup>†</sup>) and the equation was  $y = 1185.25 + 5.91 \times 10^7 x$ . The results are shown in Table 2.

Among current responsive drug delivery systems, pH is one of the most popular stimuli and has been explored extensively. As shown in Fig. 8(a)–(c), the fluorescence intensity of Nile red encapsulated in micelles significantly reduced in the function of time in acidic environment. By comparing fluorescence emission intensities at 620 nm in Fig. 7d, we found that the relative fluorescence intensity decreased to 80.01%, 58.73% and 32.21% within 20 min in pH 6.5, 6.0 and 5.5, respectively. In addition, the relative intensity decreased to 67.70%, 51.37% and 26.82% within 140 min in various pH environment. These results indicate that the acid environment can induce the efficient release hydrophobic model molecule encapsulated in micelles. And the release rate and efficiency increase as the acidity increases. This phenomenon is attributed to the sensitive pH-responsive property of polymeric micelles.

The reduction-responsive property of polymeric micelle endows it steady release the loaded hydrophobic model molecule. As shown in Fig. 9, the relative fluorescence intensity at

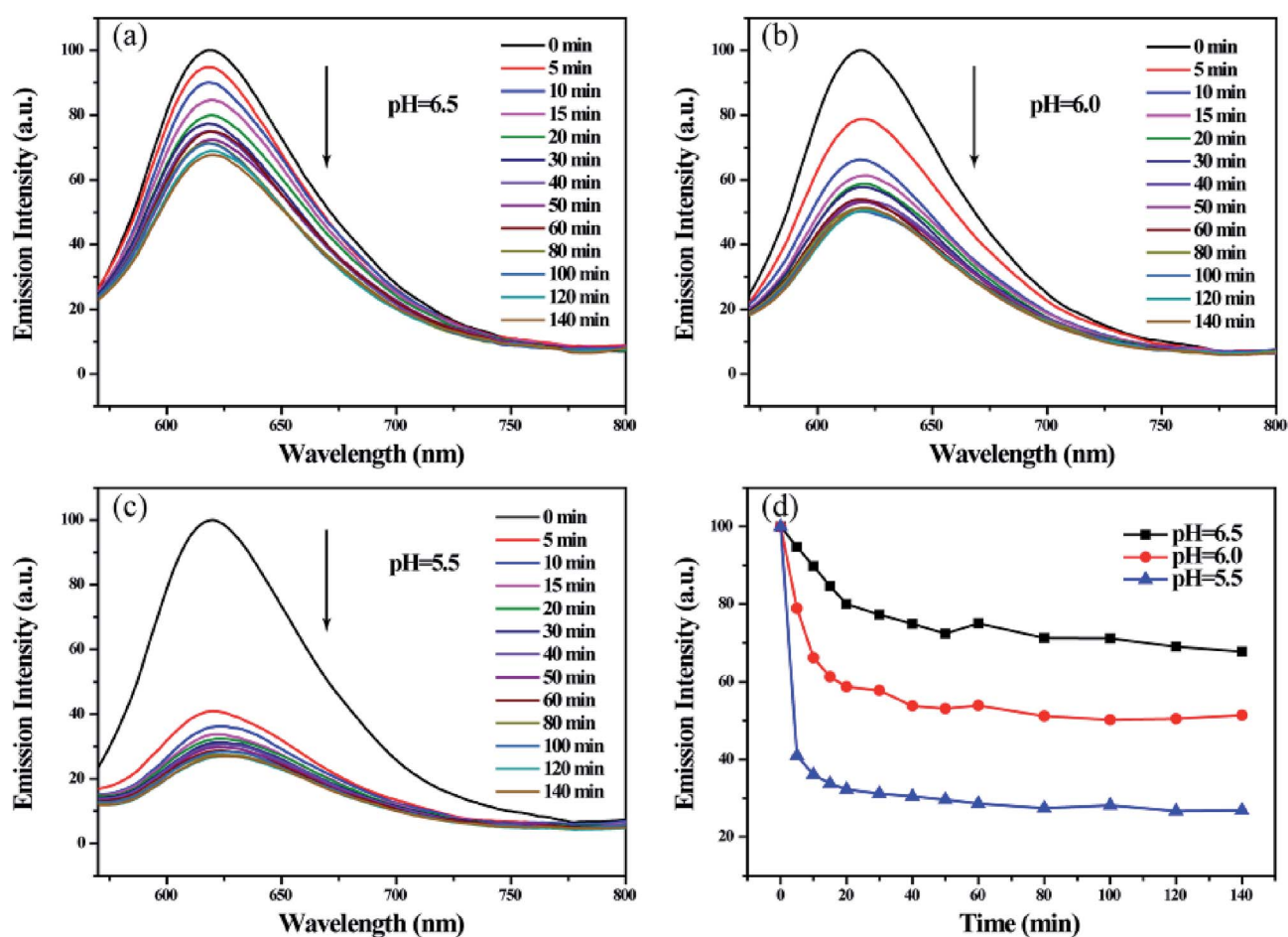


**Fig. 8** Fluorescence emission spectra of Nile red encapsulated micelle solutions (a)–(c) and the relationship between  $I_{620\text{ nm}}$  and time (d) on treatment with various pH.



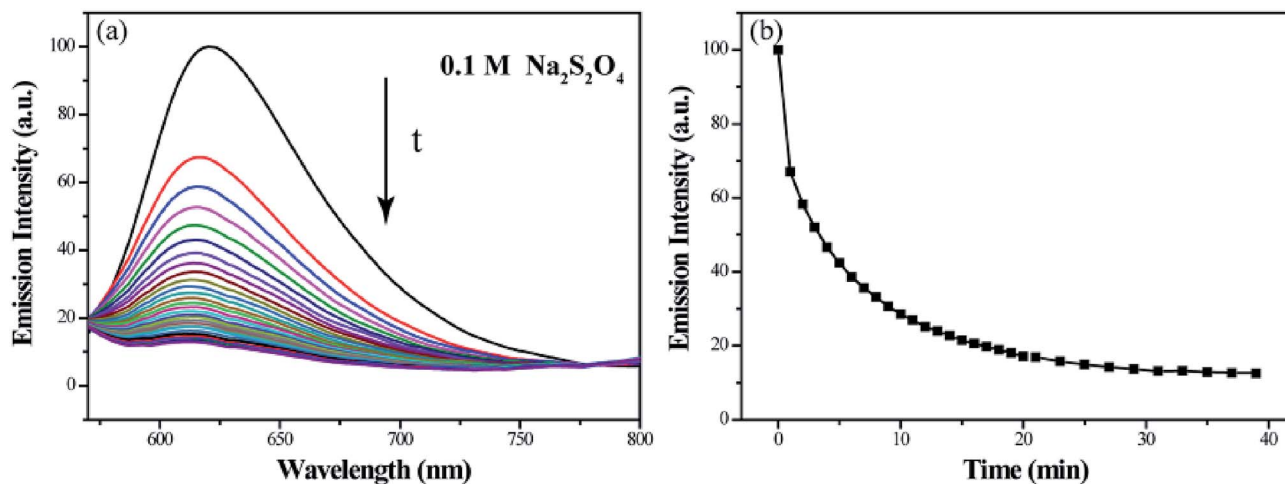


Fig. 9 Fluorescence emission spectra of Nile red encapsulated micelle solutions (a) and the relationship between  $I_{620\text{ nm}}$  and time (b) on treatment with Na<sub>2</sub>S<sub>2</sub>O<sub>4</sub> aqueous solution.

620 nm of Nile red decreases to 17.1% within 20 min and 12.5% within 39 min, demonstrating that the most of model molecule encapsulated in micelles can be released into water after adding Na<sub>2</sub>S<sub>2</sub>O<sub>4</sub>. This steady release property can be explained by the disassembly of micelles in a reductive environment.

## 4. Conclusions

In this paper, we synthesized a series of azobenzene-based copolymers, P(POSSMA-*co*-AZOMA-*co*-DMAEMA) via RAFT polymerization. In this way, the light and reduction dual-responsive azo group, pH-responsive tertiary amine group and super hydrophobic POSS moiety were incorporated into the polymer chain to generate multi-stimuli-responsive amphiphiles. The effects of initial concentration and molecular weight on micellar morphology and size were investigated by TEM and DLS and revealed that the sizes of micelles tend to increase as the concentration or molecular weight increases. The azo groups can undergo *trans*-*cis* isomerization under UV light irradiation and the diameters of micelles decreased. Owing to the large proportion of tertiary amine groups in amphiphiles, the micelles showed sensitive pH-responsive property. Hydrophobic azo pendant in polymer chain completely reduced to the corresponding more hydrophilic substituted anilines in a reductive environment, resulting in the increase of overall hydrophilicity of amphiphiles and the disassembly of polymeric micelles. Based on the pH- and reductive-stimuli-responses of micelles, we explored the release properties of self-assembly micelles by fluorescence spectroscopy. As expected, the acid or reducing environment can induce the rapid and efficient release of hydrophobic molecules loaded in micelles. Hence, as a novel azobenzene-based amphiphiles with distinctive virtues, these multi-stimuli-responsive P(POSSMA-*co*-AZOMA-*co*-DMAEMA) copolymers are potentially used for many applications in biotechnology, especially in drug control release for targeted therapy.

## Conflicts of interest

There are no conflicts to declare.

## Acknowledgements

The authors acknowledge the National Natural Science Foundation of China (51273164, 51573150) for funding. Financial support from Scientific, Xiamen Science and Technology Major Project (3502Z20171002), and Technological Innovation Platform of Fujian Province (2014H2006) is also gratefully acknowledged.

## References

- 1 S. Davaran, A. Ghamkhari, E. Alizadeh, B. Massoumic and M. Jaymand, *J. Colloid Interface Sci.*, 2017, **488**, 282–293.
- 2 X. L. Zhao, W. G. Liu, D. Y. Chen, X. Z. Lin and W. L. Willian, *Macromol. Chem. Phys.*, 2007, **208**, 1773–1781.
- 3 Q. Jin, G. Y. Liu, X. S. Liu and J. Ji, *Soft Matter*, 2010, **6**, 5589–5595.
- 4 D. Y. Xia, G. C. Yu, J. Y. Li and F. H. Huang, *Chem. Commun.*, 2014, **50**, 3606–3608.
- 5 W. L. Zhang, J. L. He, Z. Liu, P. H. Ni and X. L. Zhu, *J. Polym. Sci., Polym. Chem. Ed.*, 2010, **48**, 1079–1091.
- 6 S. J. T. Rezaei, H. S. Abandansari, M. R. Nabid and H. Niknejad, *J. Colloid Interface Sci.*, 2014, **425**, 27–35.
- 7 L. L. Chang, J. J. Liu, J. H. Zhang, L. D. Deng and A. J. Dong, *Polym. Chem.*, 2013, **4**, 1430–1438.
- 8 K. T. Chung, S. E. Stevens and C. E. Cerniglia, *Crit. Rev. Microbiol.*, 1992, **18**, 175–190.
- 9 W. M. Koppes, J. S. Moran, J. C. Oxley and J. J. Smith, *Tetrahedron Lett.*, 2008, **49**, 3234–3237.
- 10 L. B. Wang, X. Q. Pan, Y. Zhao, Y. Chen, W. Zhang, Y. F. Tu, Z. B. Zhang, J. Zhu, N. C. Zhou and X. L. Zhu, *Macromolecules*, 2015, **48**, 1289–1295.



- 11 W. M. Koppes, J. S. Moran, J. C. Oxley and J. L. Smith, *Tetrahedron Lett.*, 2008, **49**, 3234–3237.
- 12 Y. Y. Yang, M. Grammel, A. S. Raghavan, G. Charron and H. C. Hang, *Chem. Biol.*, 2010, **17**, 1212–1222.
- 13 X. Y. Hu, K. K. Jia, Y. Cao, Y. Li, S. Qin, F. Zhou, C. Lin, D. G. Zhang and L. Y. Wang, *Chem.–Eur. J.*, 2015, **21**, 1208–1220.
- 14 S. Yadav, S. R. Deka, G. Verma, A. K. Sharma and P. Kumar, *RSC Adv.*, 2016, **6**, 8103–8117.
- 15 A. Luciano, M. Benedini, A. Sequeira, M. L. Fanani, B. Maggio and I. D. Verónica, *J. Phys. Chem. B*, 2016, **120**, 4053–4063.
- 16 D. Manna, T. Udayabhaskararao, H. Zhao and R. Klajn, *Angew. Chem., Int. Ed.*, 2015, **54**, 12394–12397.
- 17 W. Qiang, L. Zhen, T. Qian, G. B. Cheng, M. H. W. Lam, X. M. Ma and C. F. Chow, *J. Mol. Recognit.*, 2016, **29**, 123–130.
- 18 J. Dong, R. Zhang, X. Zhan, H. Yang, S. Zhu and G. Wang, *Polym. Sci.*, 2014, **39**, 781–815.
- 19 H. Finkelmann, E. Nishikawa, G. G. Pereira and M. Warner, *Phys. Rev. Lett.*, 2001, **87**, 015501.
- 20 A. Sanchez-Ferrer, A. Merekalov and H. Finkelmann, *Macromol. Rapid Commun.*, 2011, **32**, 671–678.
- 21 J. F. Gohy and Y. Zhao, *Chem. Soc. Rev.*, 2013, **42**, 7117–7129.
- 22 G. J. Wang, D. Yuan, T. T. Yuan, J. Dong, N. Feng and G. X. Han, *J. Polym. Sci., Polym. Chem. Ed.*, 2015, **53**, 2768–2775.
- 23 D. Hu, Y. F. Li, Y. L. Niu, L. Li, J. W. He, X. Y. Liu, X. N. Xia, Y. B. Lu, Y. Q. Xiong and W. J. Xu, *RSC Adv.*, 2014, **4**, 47929–47936.
- 24 J. Y. Rao, C. Hottinger and A. Khan, *J. Am. Chem. Soc.*, 2014, **136**, 5872–5875.
- 25 X. M. Li, J. Y. Li, Y. Gao, Y. Kuang, J. F. Shi and B. Xu, *J. Am. Chem. Soc.*, 2010, **132**, 17707–17709.
- 26 Y. H. Xue, H. X. Wang, D. S. Yu, L. F. Feng, L. M. Dai, X. G. Wang, T. Lin and L. Tong, *Chem. Commun.*, 2009, 6418–6420.
- 27 E. R. Chan, A. Striolo, C. McCabe and P. T. Cumming, *J. Chem. Phys.*, 2007, **127**, 114102.
- 28 K. Zeng and S. X. Zheng, *J. Phys. Chem. B*, 2007, **111**, 13919–13928.
- 29 Q. Y. Guo, P. T. Knight and P. T. Mather, *J. Controlled Release*, 2009, **137**, 224–233.
- 30 Z. Y. Zhou, L. M. Cui, Y. Zhang, Y. U. Zhang and N. W. Yin, *Eur. Polym. J.*, 2008, **44**, 3057–3066.
- 31 L. Lu, C. U. Zhang, L. H. Li and C. R. Zhou, *Carbohydr. Polym.*, 2013, **94**, 444–448.
- 32 Y. T. Xu, J. M. Huang, Y. T. Li, M. J. Wang, Y. Cao, C. H. Yu, B. R. Zeng and L. Z. Dai, *Macromol. Res.*, 2017, **25**, 817–825.
- 33 L. Ma, H. P. Geng, J. X. Song, J. Z. Li, G. X. Chen and Q. F. Li, *J. Phys. Chem. B*, 2011, **115**, 10586–10591.
- 34 L. Matějka, M. Janta, J. Pleštil, Z. Alexander and M. Šlouf, *Polymer*, 2014, **55**, 126–136.
- 35 M. S. Ho, A. Natansohn, C. Barrett and P. Rochon, *Can. J. Chem.*, 1995, **73**, 1773–1778.
- 36 L. Li, K. Raghupathi, C. Song, P. Prasad and S. Thayumanavan, *Chem. Commun.*, 2014, **50**, 13417–13432.

